

BCMB 8020  
April 13,2006

•Nucleotides Sugars

- Nucleotide Sugar Transporters
- Glycosyltransferases

NUCLEOTIDE SUGARS

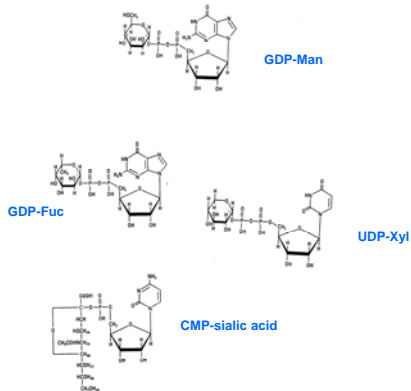
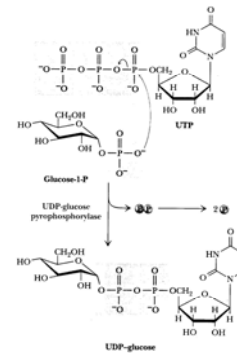
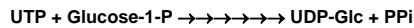
Nucleotide sugars: high energy cosubstrates involved in carbohydrate biosynthetic reactions. The energy of the hemiacetal phosphate allows nucleotide sugars to donate the sugar residue to a suitable acceptor with the concomitant release of UDP.

Nucleotide sugars are glycosyl-group donors for the glycosyltransferases that synthesize N- and O-linked oligosaccharide chains of glycoproteins; proteoglycans; glycosaminoglycans; cell wall polysaccharides; lipopolysaccharides; capsular polysaccharides; and that catalyze the glycosylation of metabolites in the cell.

Nucleotide sugars are produced in the cytosol (most nucleotide sugars) or in the nucleus (CMP-sialic acid)

Nucleotide sugars can be formed by the action of specific nucleotide sugar pyrophosphorylases (e.g. UDP-glucose pyrophosphorylase, see Fig 21.22)

UDP-Glc pyrophosphorylase

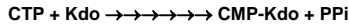


\*\* Kdo (2-keto-3-deoxy-manno-octonic acid) and sialic acid are unique since they are activated by coupling to monophospho- rather than to the usual diphosphonucleosides. Dha (3-deoxy d-lyxo-2-heptulosaric acid) may be activated in a similar fashion.

Kdo is a component of lipopolysaccharides in Gram-negative bacteria and in the pectic polysaccharide rhamnogalacturonan II in plant cell walls.

**CMP—Kdo synthetase (L-CKS)** (kdsB gene, E.coli) catalyzes synthesis of CMP-Kdo for use in synthesis of lipopolysaccharides:

CKS; Mg<sup>2+</sup>



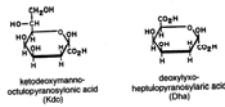
Pathogenic E.coli with group II capsular polysaccharides synthesize a 2nd CKS gene called K-CKS (kpsU). K-CKS has 245 amino acids & is 44% identical to L-CKS.

Due to rapid spread of antibiotic resistance in bacteria strains, & because mammals do not make K-CKS, it is a target for drug design. Thus, kpsU was cloned, overexpressed, purified, crystallized & X-ray structure determined. This is the **1st structure of a sugar-activating enzyme**.

Enzyme is homodimer with subunits of 27,028 daltons. Each subunit has a seven-stranded parallel β-sheet flanked on both sides by α helices.



Fig. 4. Ribbon plot of one subunit of the dimeric capsular-specific CMP-Kdo synthetase produced with MOCSKOPT [16]. Residues are given as sticks and beta-sheets as arrows. The nucleotide binding site is a β-strand loop. Arg-18 and Lys-19 are depicted together with the KCS<sup>+</sup> cation in a phosphate binding site.



In **plants nucleotide sugars** can be grouped into:

**“Primary nucleotide sugars”** (ADP-Glc, TDP-Glc, UDP-Glc, UDP-GlcNAc and GDP-Man). These nucleotide sugars are synthesized by pyrophosphorolysis from the corresponding glycosyl phosphates that are formed directly from fructose-6-P produced via photosynthesis.

**“Secondary nucleotide sugars”** (UDP-Gal, UDP-GlcA, UDP-GalA, UDP-Xyl, UDP-Ara, TDP-Glc, GDP-Man, ADP-GlcNAc, GDP-Fuc, CDP-Glc, GDP-Glc) are formed by enzymatic **modification** (nucleotide-sugar transformations) of the **glycosyl moieties** of the primary nucleotides or from the action of pyrophosphorylases that function in the salvage pathway. Monosaccharides released during seed germination, from the wall, etc., are degraded into monosaccharides, phosphorylated by kinases, and converted to nucleotide sugars by pyrophosphorylases.

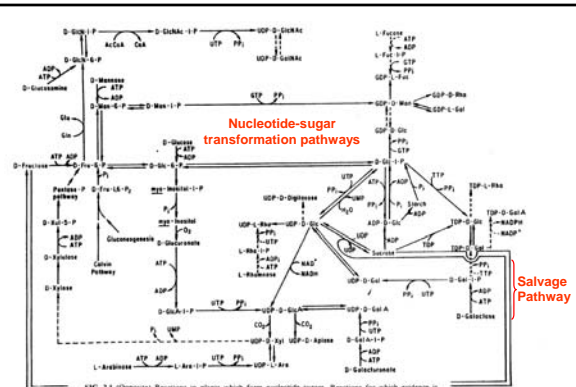


FIG. 2.1 (Opposite) Reactions in plants which form nucleotide sugars. Reactions for which evidence is fragmentary or preliminary are shown by dashed lines. The direction in which the reaction is most likely to proceed under normal physiological conditions is indicated by the arrows. First xylanase, D-galactinase, D-glucanase, D-galacturonase, and D-cytase result from the hydrolytic degradation of complex polysaccharides or sugar phosphates. D-glucosamine also is formed by oxidation of D-glucosamine in the associated osidation pathway.

**UDP-Galactose 4-epimerase** catalyzes the reversible conversion of UDP-Gal to UDP-Glc. The enzyme from *E. coli* is a homodimer of MW 79,000. The *E. coli* enzyme contains noncovalently bound NAD<sup>+</sup>. The epimerization involves the transient oxidation/reduction in which a hydride is removed from the 4 position of the UDP-sugar & returned to the opposite face of the enzyme-bound 4-ketopyranose intermediate. Each subunit binds UDP-sugar & NAD<sup>+</sup>.

**2 Domains**

N-terminal domain (1-180), NAD<sup>+</sup>-binding motif (7 strands  $\beta$  sheet flanked by  $\alpha$  helices)  
C-terminal domain (181-338), active site at cleft between domains



10 strands  $\beta$  sheet  
11  $\alpha$  helices

Fig. 5. Ribbon drawing of one subunit of epimerase, generated using software kindly provided by Dr. J. P. Prestige. Strands of  $\beta$ -pleated sheet are shown as arrows, while  $\alpha$ -helices are shown as coils. Each epimerase subunit contains 10 strands of  $\beta$ -pleated sheet, and 11  $\alpha$ -helices.

**UDP-Benzene NAD<sup>+</sup>**

**X-RAY STRUCTURE OF UDP-GALACTOSE 4-EPIMERASE**

379



Fig. 6. Stereo drawing of one subunit of epimerase. For the sake of simplicity, only the positions of the backbone  $\alpha$ -carbons are represented. The NAD<sup>+</sup> cofactor and the UDP-benzene are shown as atomic models. Various amino acid residues are labeled

to aid the reader in following the course of the polypeptide chain. The plot was generated with the software package Rvnto, originally written by Dr. Sam Moras and modified for proteins by Dr. Eleanor Dodson and Dr. Phil Evans.

**X-RAY STRUCTURE OF UDP-GALACTOSE 4-EPIMERASE**

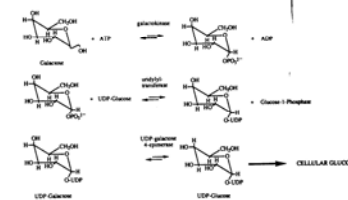


Fig. 1. Lactic pathway for the conversion of galactose to glucose. In this metabolic pathway, galactose is first converted to galactose-1-phosphate by the action of galactokinase and then to UDP-galactose by the enzyme, uridylyltransferase. Subsequently, epimerase, the enzyme described in this report, converts UDP-galactose to UDP-glucose as shown.

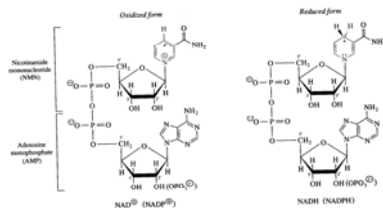


Figure 7-8 Oxidized and reduced forms of NAD (and NADP). The pyridine ring of NAD<sup>+</sup> is reduced by addition of a hydride ion to C-4 when NAD<sup>+</sup> is converted to NADH (and when NADP<sup>+</sup> is converted to NADPH). In NADH, the 2'-hydroxyl group of the sugar ring of adenine is phosphorylated. The reactive center of these coenzymes is shown in red.

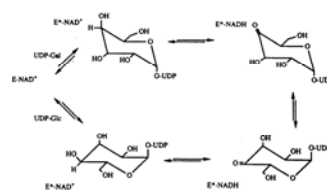


Fig. 2. Possible mechanism for epimerase action. From Frey,<sup>7</sup> a putative 4-ketopyranose intermediate. Subsequently, there is a rotation of the 4-ketoglucose moiety around the glycosyl oxygen  $\beta$ -phosphorus bond thus altering the face of the intermediate which is available for hydride return.

BCMB 8020  
April 13,2006

- Nucleotides Sugars
- Nucleotide Sugar Transporters**
- Glycosyltransferases

### Nucleotide-Sugar Transporters

Integral-membrane proteins that transport specific nucleotide sugar from the cytosol into a membrane bound compartment

Evidence that nucleotide-sugars are transported by specific transporters

- \* no competition for transport by different nucleotide-sugars
- \* nucleotide-sugar mutants: the mutation is specific for a specific nucleotide sugar

Nucleotide-sugar transporters are found in both the ER and Golgi membrane

Nucleotide-sugar transporters found in the Endoplasmic Reticulum

UDP-GlcNAc, UDP-GalNAc, UDP-Xyl, UDP-GlcA, UDP-Glc, (ATP)

Nucleotide-sugar transporters found in the Golgi

CMP-SA, UDP-Gal, GDP-Fuc, UDP-GlcNAc, UDP-GalNAc, UDP-Xyl, UDP-GlcA, UDP-GalA (plants), UDP-GlcA, UDP-Glc, GDP-Man (yeast & Leishmania), (PAPS;3'-phosphoadenosine 5'-phosphosulfate), (ATP)

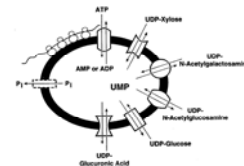


Figure 2. Nucleotide-sugar and ATP transporters in the endoplasmic reticulum have been identified in mammals and yeast. These are associated with the corresponding nucleotide phosphorylation using the ATP when ADP or AMP in both are active. The existence of an integral phosphatase transporter is hypothesized.

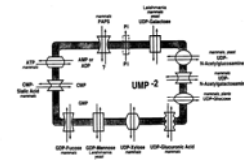


Figure 3. Golgi membrane nucleotide sugar, ATP, and PAPS transporters have been identified in mammals and yeast. These are associated with the corresponding nucleotide phosphorylation using the ATP when ADP or AMP in both are active. The existence of an integral phosphatase transporter is hypothesized.

The transport of nucleotide-sugars into the Golgi is:

Saturable

Sensitive to proteolysis at cytoplasmic side of membrane

Temperature dependent (little transport at 0°-4°C)

Antiport with NMP

NDP-sugar2-:NMP2- exchange is electroneutral

*Example:* UDP-GlcNAc transport across rat liver Golgi membranes. Waldman, B.C. & Rudnick, G. (1990) Biochemistry 29:44-52

Km 7.13 ± 1.62 μM; Vmax: 915 ± 87 pmol mg<sup>-1</sup> min<sup>-1</sup>. Activity at 0°C 7.6% of that at 30°C.

(Note: pKa for UDP-GlcNAc -2; pKa for monoanionic to dianionic from of UMP is 6.4)

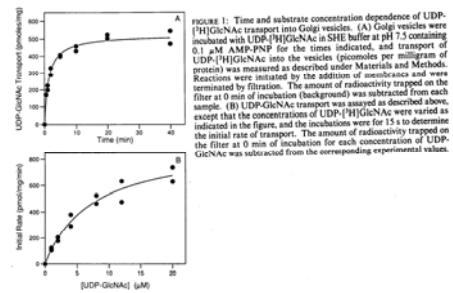
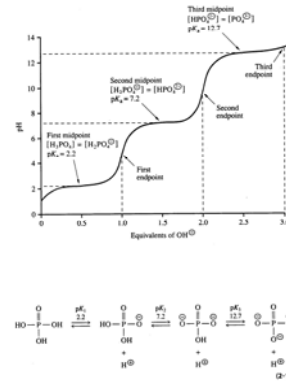


FIGURE 1. Time and substrate concentration dependence of UDP-[<sup>3</sup>H]GlcNAc transport into Golgi vesicles. (A) Golgi vesicles were incubated with UDP-[<sup>3</sup>H]GlcNAc in SHE buffer at pH 7.5 containing 0.1 μM AMP-PNP for the times indicated, and transport of UDP-[<sup>3</sup>H]GlcNAc into the vesicles (picomoles per milligram of protein) was measured as described under Materials and Methods. Reactions were initiated by the addition of membranes and were terminated by filtration. The amount of radioactivity trapped on the filter at 0 min of incubation (background) was subtracted from each sample. (B) UDP-GlcNAc transport was assayed as described above, except that the concentrations of UDP-[<sup>3</sup>H]GlcNAc were varied as indicated in the figure, and the incubations were for 15 s to determine the initial rate of transport. The amount of radioactivity trapped on the filter at 0 min of incubation for each concentration of UDP-GlcNAc was subtracted from the corresponding experimental values.

**Table II: Effect of Internal and External pH on UDP-GlcNAc Transport into UMP-Loaded Vesicles\***

internal pH	initial rate of transport (pmol mg <sup>-1</sup> min <sup>-1</sup> ) for external pH of	
	5.45	7.50
5.45	28.98 (±38.20) <sup>b</sup>	56.24 (±81.06)
7.50	516.08 (±7.64)	367.62 (±42.15)

\*Standard deviation. <sup>b</sup>Golgi vesicles were mechanically loaded with either SME buffer at pH 5.45 or SHE buffer at pH 7.50, both containing 6 mM AMP-PNP (to prevent degradation of the UMP) and with or without 1 mM UMP, as described under Materials and Methods. Samples (2 μL containing 40–50 μg of protein) were assayed for 15 s to measure the initial rate of UDP-[<sup>3</sup>H]GlcNAc transport as described under Materials and Methods. The external medium (200 μL) was similarly buffered at either pH 5.45 or pH 7.50, as indicated, and contained 1 μM AMP-PNP. The values represent the average of duplicates, after the subtraction of the corresponding buffer-loaded (without UMP) background values.



**Transport of nucleotide sugars by nucleotide-sugar transporters**

Km for nucleotide-sugar is 1-10 μM

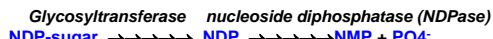
Ki for NMP is 1-5 μM

Transporter inhibited by: NDP, NTP, deoxy-nucleotides

Not inhibited by: nucleoside 2' & 3'-phosphates or by free sugar

Transporters have MW ~ 30-40 kD

Fate of NDP-sugar once transferred into the membrane organelle.



Note: Golgi luminal GDPase in yeast functions as a homodimer in the membrane

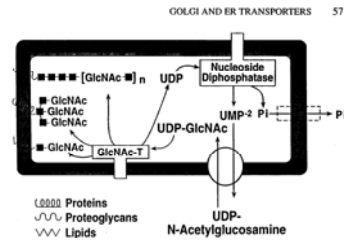
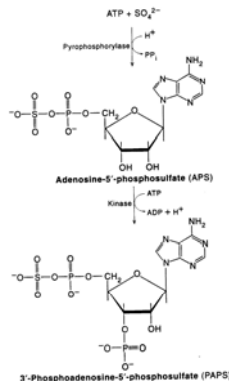


Figure 7 Mechanism of mammalian Golgi membrane transporters. UDP-N-acetylglucosamine is transported into the lumen of the Golgi apparatus, where N-acetylglucosamine is transferred to proteins, proteoglycans, and lipids in reactions catalyzed by specific N-acetylglucosaminyltransferases. UDP, the other reaction product, is converted by a luminal nucleoside diphosphatase to UMP-2<sup>-</sup> and inorganic phosphate. The latter is postulated to exit the Golgi lumen via a specific transporter.



NDP-sugars transporters can be solubilized from the membranes and reconstituted in proteoliposomes. The kinetic properties of the reconstituted transporters are similar to their properties in intact Golgi.

The PAPS transporter (e.g. required for sulfation of glycosaminoglycans) was purified by reconstitution assays, but the purification of nucleotide transporters using this approach has proven difficult due to the low levels present in cells.

Nucleotide –sugar transporters have been cloned based on complementation of mutants. Transporters for UDP-Gal, UDP-GlcNAc, GDP-Man, CMP-sialic acid have been cloned.

**Example:** Cloning of UDP-GlcNAc transporter from *Kluyveromyces lactis* (Abejon, C., Robbins, P.W., and Hirschberg, C.B., 1996, PNAS 93:5963-5968)

A mutant on the yeast *Kluyveromyces lactis* (*mnn2-2*) produces mannoproteins without a terminal GlcNAc residue, are impaired in the biosynthesis of GlcN containing lipids, have normal levels of N-acetylglucosaminyltransferase activity. **Proof that the mutant was defective in the transport of UDP-GlcNAc into Golgi vesicles:** The initial rate of transport of UDP-GlcNAc into Golgi vesicles from wild-type cells was temperature dependent, saturable with an apparent  $K_m$  of 5.5  $\mu M$  and a  $V_{max}$  of 2.7  $pmol\ mg^{-1}\ min^{-1}$ . **No transport of UDP-GlcNAc was detected into Golgi vesicles from mutant cells.** However, Golgi vesicles from both cells translocated GDP-mannose at comparable velocities, indicating that the above transport defect is specific.

The gene for the UDP-GlcNAc transporter was cloned by **complementing the *mnn2-2* mutation.**

Genomic library from wild type *Kluyveromyces lactis* was transformed into the *mnn2-2* mutant. Transformants selected by phenotypic correction (i.e. expression of the GlcNAc on the mannoproteins on the cell surface) by labeling with a fluorescein conjugated lectin.

**Lectins:** carbohydrate binding proteins specific for specific carbohydrate(s)

(Methods note: *Nucleotide sugar-transporter mutants can be identified based on their sensitivity to lectins*)

*Griffonia simplicifolia* II lectin binds terminal GlcNAc residues.

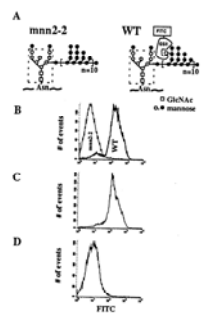


FIG. 1. Cell surface labeling and separation of *K. lactis* cells by FACS. (A) Mannan chains of mutant *K. lactis* (*mnn2-2*) and wild-type *K. lactis* cells. Terminal N-acetylglucosamine on the wild-type chains binds to GS II-FITC lectin. (B) Fluorescence emission of mutant *K. lactis* (*mnn2-2*) and wild-type *K. lactis* cells following GS II-FITC lectin binding and FACS. (C) Fluorescence emission of *K. lactis* cells transformed with pGAL-URA1-MNN2-2. (D) Fluorescence emission of transformant of C after plating on 5-fluorouracil (loss of plasmid) and labeling with GS II-FITC lectin.

### Primary structure of nucleotide-sugar transporters

Nucleotide-sugar transporters that have been cloned:

- UDP-Gal
- UDP-GlcNAc
- GDP-Man
- CMP-sialic acid

Nucleotide-sugar transporters encode proteins of ~320-400 amino acids that are 40-60% similar in aa sequence. They are very hydrophobic, integral membrane proteins with 5-9 putative transmembrane domains. Some transporters have leucine zipper motif sequences (i.e. possible oligomerization signals) and N-linked glycosylation sites, but the significance of both motifs/sites is not clear.

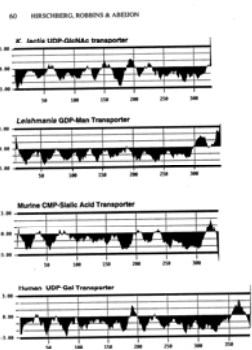


Figure 3. Key doublet hydrophobicity plots of the Golgi membrane nucleotide sugar transporters (GLT1, GLN1, and GLY1, respectively). Underline and box indicate sites.

### Nucleotide Sugar Transporters, the Present and the Future



Fig. 5. The possible structure of human UDP-galactose transporter 1 (hGLT1) inferred with the program, TMAP (22). The columns represent putative transmembrane domains. The four leucine residues representing the leucine zipper motif are underlined, and conservative residues representing potential glycosylation sites are boxed. Lollipop indicate possible protein kinase C phosphorylation sites.

Golgi lumen

- Nucleotides Sugars
- Nucleotide Sugar Transporters
- **Glycosyltransferases**

**GLYCOSYLTRANSFERASES: Structure, Localization, and Control of Cell-Type-Specific Glycosylation (1989)**  
 J. Biol. Chem. 264:17615-17618

**Glycosyltransferases:** transfer sugar residues from an activated sugar donon (usually nucleotide-sugar) to a growing carbohydrate group

≥100 **glycosyltransferases** are required to synthesis glycoproteins & glycolipids in animals

“It is likely that common terminal sequences of **glycoprotein** and **glycolipid** sugar chains are synthesized by the same glycosyltransferases”

**Glycosyltransferases** share no (or little) sequence homology, but do have a common domain structure:

- \*Short NH2-terminal cytoplasmic tail
- \*16-20 amino acid signal-anchor domain
- \*extended stem region
- \*large COOH-terminal catalytic domain

Many **Glycosyltransferases** are Type II membrane proteins (i.e. N-terminus is on the cytosolic side, C-terminus on the luminal side)

Most of the transferases show little apparent sequence homology. Comparison of a number of cloned glycosyltransferases has revealed a short motif that contains two Asp residues (DXD) that is thought to be part of the catalytic site (see Wiggins, C.A.R. and Munro, S., 1998, PNAS 95:7945-7950)

TABLE I  
 Cloned glycosyltransferases involved in the synthesis of terminal sequences in sugar chains of glycoproteins and glycolipids  
 Abbreviated names combine the acceptor sugar, the linkage formed, and the glycosyltransferase family (GT, galactosyltransferase; ST, sialyltransferase; FT, fucosyltransferase; GaNAcT, N-acetylglucosaminyltransferase). For the acceptor formed, the sugar transferred is highlighted in boldface, and the acceptor sequence is shown in lightface. R represents the remainder of the glycoprotein or glycolipid sugar chain.

GLYCOSYL-TRANSFERASE	DONOR SUBSTRATE	SEQUENCE FORMED
<b>Galactosyltransferases</b>		
GalNAc 3-GT (19-15) (E.C. 2.4.1.36)	UDP-Gal	Galβ1AGlcNAc-R
Gal α1-3-GT (16,17) (E.C. 2.4.1.37)	UDP-Gal	Galα1-3Galβ1-4GlcNAc-R
<b>Sialyltransferase</b>		
Gal α1-6-ST (18) (E.C. 2.4.99.5)	CMP-NeuAc	NeuAcα6Galβ1-4GlcNAc-R
<b>Fucosyltransferases</b>		
GalNAc α1-3-FT <sup>1</sup> (E.C. 2.4.1.45)	GDP-Fuc	Fucα1-3GalNAc-R Fucα1-4GalNAc-R Fucα1-6GalNAc-R Fucα1-3GlcNAc-R
Gal α1-2-FT <sup>1</sup> (E.C. 2.4.1.46)	GDP-Fuc	Fucα1-2Galβ1-4GlcNAc-R Fucα1-2Galβ1-3GlcNAc-R
<b>N-Acetylglucosaminyl-transferase</b>		
Gal α1-2-GalNAcT <sup>2</sup> (short gap A member)	UDP-GalNAc	GalNAcα1-2Gal-R Fucα1-2

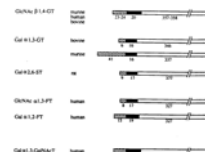


FIG. 1. Amino acid sequences of cloned terminal glycosyltransferases predict N16-terminal signal-anchor domains. Compared are the predicted domain structures of six glycosyltransferases listed in Table I. The number of amino acids in each domain is listed beneath it. E, cytoplasmic domain; S, signal-anchor domain; C, luminal domain.

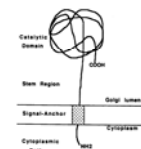
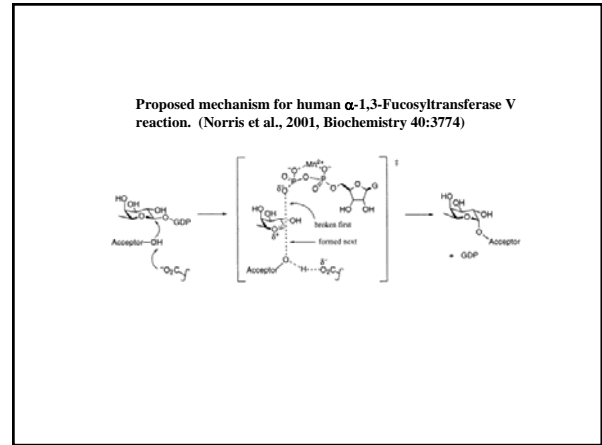
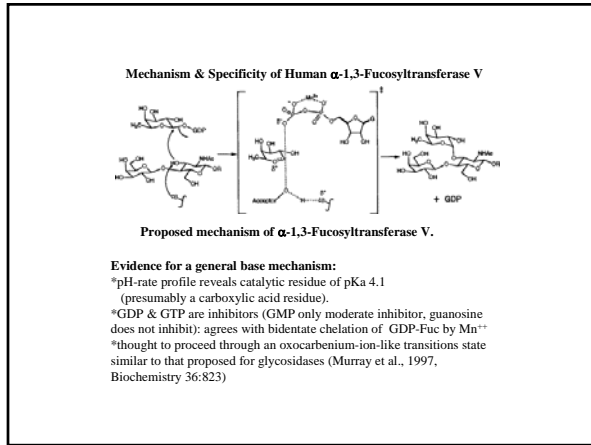
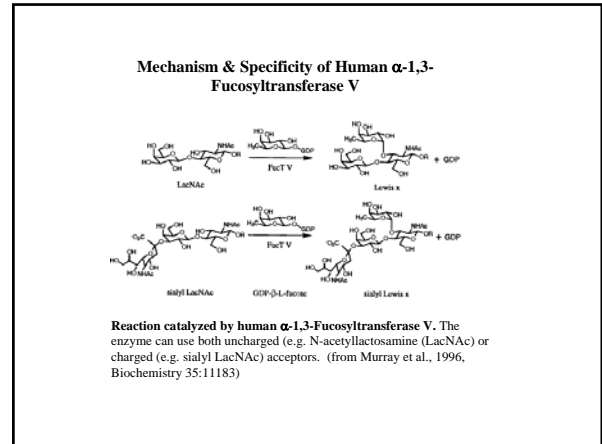
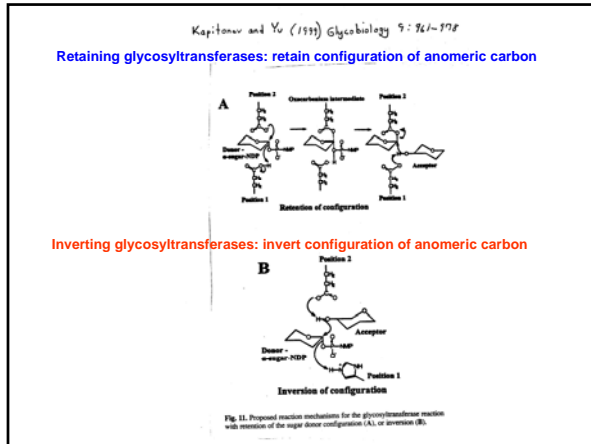
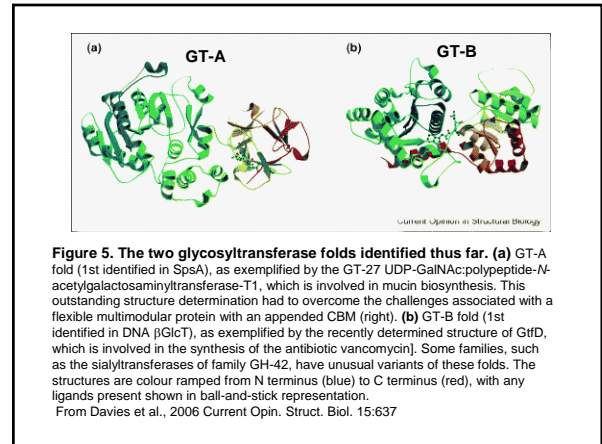


FIG. 2. Common topology of cloned terminal glycosyltransferases. Deduced amino acid sequences of the terminal glycosyltransferases cloned to date predict that these enzymes have a characteristic topology in the Golgi apparatus consisting of a short N16-terminal cytoplasmic tail, a signal anchor domain which spans the membrane, an extended stem region, and a large COOH-terminal catalytic domain situated within the lumen of the Golgi cisternae.



- Based on glycosyltransferase crystal structures: two superfamilies are proposed.**
- **GT-A (SGC) superfamily:** (SpsA, GnTI core domain,  $\beta$ 4GalT, GicAT1).
  - All members, although sharing no significant sequence similarity, have a structurally very similar catalytic domain.
  - All enzymes bind their NDP-sugar in the fold between helix3 and the central  $\beta$  sheet.
  - All share the same catalytic base, DXD motif and metal-binding site.
  - It is suggested that all family members share a common ancestor.
  - **GT-B superfamily (BGT)glycogen phosphorylase, T4  $\beta$ GlcT, MurG)**
  - Share similar structure and conserved NDP-sugar binding site



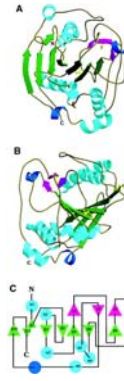
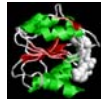
### GT-A

Two tightly associated  $\beta\alpha\beta$  domains or varying sizes with separated nucleotide and acceptor binding domains. These GTs usually have a short N-terminal cytosolic domain, a transmembrane segment, a stem region and a globular domain. Solved crystal structures from GT CAZy families 2, 6, 7, 8, 13 and 43.

### GT-B

Two similar, but less tightly associated Rossman-like  $\beta\alpha\beta$  fold domains. These GTs are usually membranes associated but usually do not have TM segment. Solved crystal structures from GT CAZy families 1, 4, 20, 28, 35, 63, 64.

Rossmann fold ( $\beta\alpha\beta$ ) is a common motif for nucleotide-binding



Overall view of the substrate-free bovine 4Gal-T1 catalytic domain structure. Crystal structure shows a new fold consisting of a single conical domain with a large open pocket at its base that interacts with the NDP-sugar. (Gastineal et al., 1999, EMBO J 18:3546)

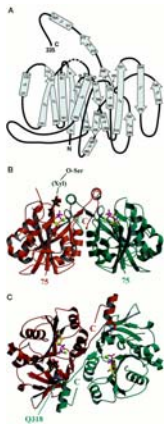
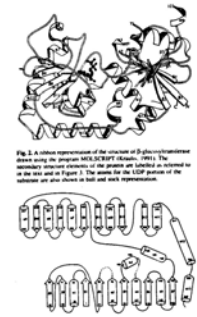


**Fig. 2.** A. Secondary structure elements of the catalytic domain (residues 75-335) of the GlcAT-I enzyme. B. Scheme of the crystallographic dimer of GlcAT-I with monomers A (orange) and B (seagreen). The UDP molecule is colored yellow, the Mn<sup>2+</sup> ion chartreuse, and the substrate in dark green. C. rotation of the crystallographic dimer by approximately 90° with respect to panel B, along a horizontal axis. In this panel residue Gln318 of one molecule extends into the active site region of the other. (Pedersen et al., 2000, J.Biol.Chem. 275:34580)

### T4 $\beta$ -GlcT transfers Glc from UDP-Glc to hydroxymethyl groups of modified cytosine in T4 duplex DNA (part of phage protection system).

Structure +/- UDP-Glc yields shift to more closed conformation



UDP-Glc binds to pocket in cleft between 2 domains

Each domain has topology reminiscent to nucleotide binding fold

### T4 $\beta$ -GlcT

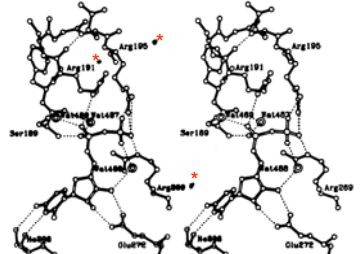


Fig. 4. A stereo view of the hydrogen bond interactions made between the UDP portion of the substrate and the surrounding protein and water molecules. The UDP portion of the substrate is shown in open bonds and the protein in closed bonds. Water molecules are shown by double circles. Hydrogen bond interactions are shown by dotted lines.

UDP has extensive H-bonding with residues in C-terminal domain  
 \*Arginine involved in making interdomain salt bridge that links UDP-Glc binding and closed conformation

### Bacillus subtilis glycosyl T (SpsA)

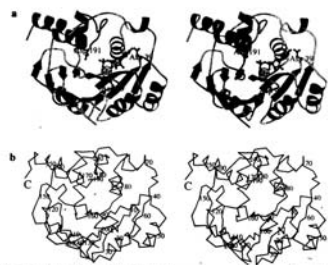


FIGURE 2. Structure of SpsA in complex with Mn-UDP. (a) In the divergent stereo cartoon representation, the UDP, Asp 99, and Asp 191 are depicted in ball-and-stick representations and the manganese ion is depicted as a shaded sphere. (b) Divergent stereo C $\alpha$  trace of SpsA with every 10th residue labeled. This figure was drawn with MOLSCRIPT (17).

